LAWRENCE
LIVERMORE
NATIONAL
LABORATORY

LLNL-JRNL-771721

On alpha-particle transport in inertial fusion

A. Zylstra, O. Hurricance

April 10, 2019

Physics of Plasmas

Disclaimer

LLNL-JRNL-771721

On alpha-particle transport in inertial fusion

A.B. Zylstra[1, a)] and O.A. Hurricane[1]
Lawrence Livermore National Laboratory

(Dated: 2 December 2020)

Analytic theory and models of inertial fusion implosion use parameterized microphysics models. In this paper we consider the DT alpha-particle transport, and report new parameterizations of the range, heating efficacy, and energy partition using modern stopping-power theory. Our resulting heating efficacy is lower than previously-published results, which reduces the temperature and pressure generated by a dynamic implosion hot-spot evolution model, and shifts the burning-plasma regime boundary slightly farther from current experimental results.

I. INTRODUCTION

The essence of controlled laboratory thermonuclear fusion is to use the fusion product's kinetic energy to self-heat the plasma, accelerating and perpetuating the burn. The Inertial Confinement Fusion (ICF) concept uses an implosion to rapidly compress and heat fuel to conditions exceeding the Lawson criterion[1,2]. In a hot-spot ICF configuration, ignition occurs in a central high-temperature low-density region, the 'hot spot', with burn subsequently propagating into a surrounding dense fuel layer to achieve high fusion gain. Hot-spot ignition is the approach currently pursued at the National Ignition Facility (NIF)[3], because it is thought to be the configuration that requires the least amount of capsule absorbed energy to reach ignition. While recent experiments have reached significant levels of self-heating[4–6] the goal of ignition remains elusive.

All such ignition schemes pursue the deuterium-tritium (DT) reaction due to its high cross section. DT fusion,

$$\mathrm{D} + \mathrm{T} \rightarrow n(14.04\ \mathrm{MeV}) + \alpha(3.54\ \mathrm{MeV}), \qquad (1)$$

primarily self-heats via the α particles energy, which is transferred to the bulk plasma at the rate at which the α loses energy as it transits the plasma, which is known as the charged-particle stopping power dE/dx. For conditions relevant to inertial fusion calculating the stopping power accurately is a theoretical challenge. Recent experimental data[7–11] has been published that indicates certain modern theories of dE/dx, particularly the Maynard-Deutsch (MD)[12,13] and Brown-Preston-Singleton (BPS)[14], are reasonably accurate at conditions relevant to ICF, with the possible exception of the lowest velocity probed in Ref. 11.

Also in recent years, the need to understand current implosions, their degradation mechanisms, and the improvements needed to reach ignition have led to a proliferation of work based on analytic or semi-analytic implosion models[4,5,15–27]. These models involve evolving the hot-spot through sources of energy gain and loss, for example writing the energy balance as

$$c_{DT}\frac{dT}{dt} = f_\alpha Q_\alpha - f_B Q_B - Q_e - \frac{1}{m}p\frac{dV}{dt} \qquad (2)$$

where dT/dt is the time derivative of hot spot temperature which depends on the DT fuel's heat capacity (c_{DT}), and the power per unit mass of α self-heating (Q_α) balanced against the loss terms from bremsstrahlung emission (Q_B), electron thermal conduction (Q_e). PdV work, the last term, can be a source or sink of energy depending on the sign of dV/dt. f_B is the fraction of bremsstrahlung x rays lost from the hot spot, and analogously f_α is the efficacy of α particle self heating, or the fraction of the DT-α energy deposited into the hot spot. Analytic theory of ICF in the literature often invokes expressions for f_α based upon simple theories of the underlying physics of charged-particle energy loss. Similarly, published expressions for the α particle's energy partition to plasma ions and electrons is also based on outdated theory.

In this paper, we present new parameterizations of the alpha particle range, stopping fraction, and energy partitioning from fits to modern stopping powers, specifically MD and BPS, which are consistent with the available experimental data. These new parameterizations can be incorporated into analytic implosion models, or data-based inferences of self-heating efficacy. This paper is organized as follows: we review the previously-published parameterizations for hot-spot energy transport in Section II, present our results for range, efficacy, and energy partition in Sections III-V, show the effect on NIF-relevant implosions in Section VI, and conclude the paper in Section VII.

II. REVIEW OF PREVIOUS FITS

A. Krokhin and Rozanov

The first parameterization of DT-α transport in ICF hot spots is due to Krokhin and Rozanov (Ref. 28). They give an α particle range λ, in length units,

$$\lambda = \frac{2.6\times10^{21}T^{3/2}}{n_e}, \qquad (3)$$

with T in keV and n_e in cm^{-3}. Equivalently, in areal density units with $\rho = 2.5n_e/N_A$,

$$\rho\lambda = 0.0108T^{3/2} \qquad (4)$$

with T in keV and $\rho\lambda$ in g/cm^2. Krokhin and Rozanov also consider the efficacy of α heating in the hot spot, f_α, which

a)Electronic mail: zylstra1@llnl.gov

they evaluate based on geometry and the range alone as

$$f_\alpha = 1 - \frac{1}{4}\frac{\rho\lambda}{\rho R} + \frac{1}{160}\left(\frac{\rho\lambda}{\rho R}\right)^3 \quad \rho\lambda/\rho R \geq 0.5$$
$$= \frac{3}{2}\frac{\rho R}{\rho\lambda} - \frac{4}{5}\left(\frac{\rho R}{\rho\lambda}\right)^2 \quad \rho\lambda/\rho R \leq 0.5 \qquad (5)$$

where ρR is the areal density of the hot spot.

B. Fraley

After Krokhin and Rozanov, Fraley et al. (Ref. 29) consider the same problem with an updated stopping power, including the effect of the plasma ions. They quote a range

$$\rho\lambda = \frac{0.015T^{5/4}}{1+0.0082T^{5/4}}, \qquad (6)$$

which is a fit assuming the plasma density is equivalent to solid DT ice, i.e. 0.213 g/cc. This is a significant underestimate of the density at conditions relevant to inertial fusion. Fraley notes that the range increases about a factor of 3 at high density (10^4 g/cc) but does not treat the density dependence in their published expressions. For the α heating efficacy they use the same geometric expression as Krokhin (Eq. 5).

Fraley also gives a fit for the fraction of α energy deposited to plasma ions, F_i,

$$F_i = \frac{1}{1+32/T_e} \qquad (7)$$

where T_e is the electron temperature in keV.

C. Atzeni

Atzeni and Meyer-ter-Vehn (Ref. 30) also treat this problem, and give an expression for the range

$$\rho\lambda = \frac{0.025T^{5/4}}{1+0.0082T^{5/4}}, \qquad (8)$$

which is equivalent to Fraley's expression (Eq. 6) multiplied by a factor of $5/3$, roughly taking into account the density dependence from solid DT ice to ICF-relevant hot spots. The geometric treatment of f_α is again equivalent to Krokhin and Rozanov. Atzeni gives a new expression for the energy partition fraction to plasma electrons as

$$F_e = \frac{28}{28+T_e}. \qquad (9)$$

D. Comparison

These three previously-published models are compared in Fig. 1. Of the three models, Atzeni's clearly has the longest calculated range ($\rho\lambda$), which corresponds to the lowest heating efficacy (f_α). This results from Atzeni's calculation at densities more relevant to modern ICF designs. We note that in the literature of analytic implosion modeling, Atzeni's expression for $\rho\lambda$ is most commonly used, although the Fraley's fit is also used, with the Krokhin-Rozanov geometric expression for f_α employed widely.

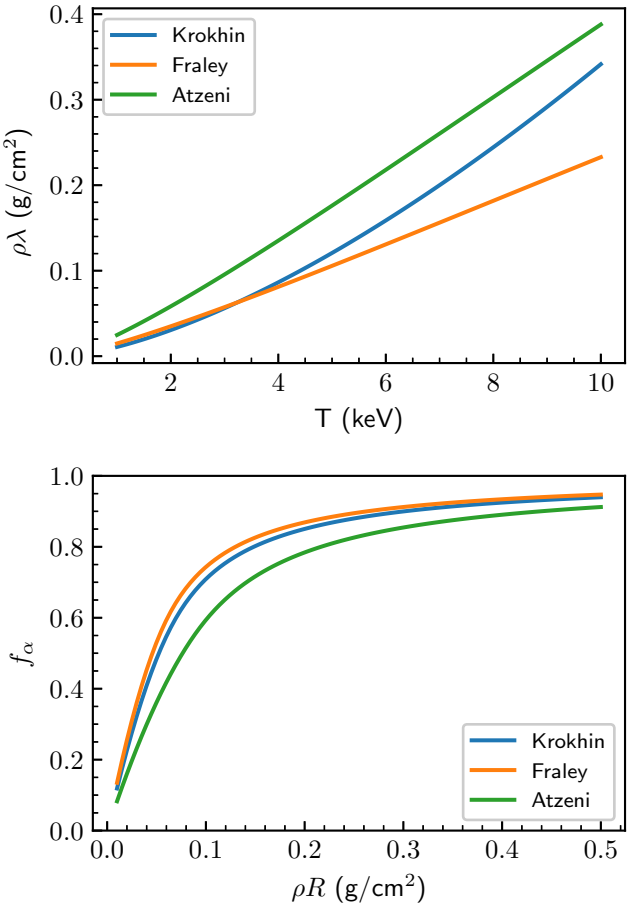

FIG. 1. Range ($\rho\lambda$, top) and heating efficacy (f_α, bottom) for the three previously-published models. f_α is evaluated at 5 keV.

III. RANGE

The range of a charged particle is straightforward to calculate given a stopping power dE/dx from the expression

$$E_0(T) = \int_0^{\rho\lambda} \frac{dE}{dx}dx, \qquad (10)$$

where E_0 is the initial α energy. Based on reaction kinematics the α birth energy is a function of temperature, with the approximate form[31]

$$E_0(T) = 3.5621 + 2.4193\times10^{-3}T + 1.9718\times10^{-5}T^2 \qquad (11)$$

with T in keV and E_0 in MeV. The α range is shown in Fig. 2 evaluated using MD (solid curves) and BPS (dashed) at 10 (blue), 50 (magenta) and 100 (red) g/cc compared to the

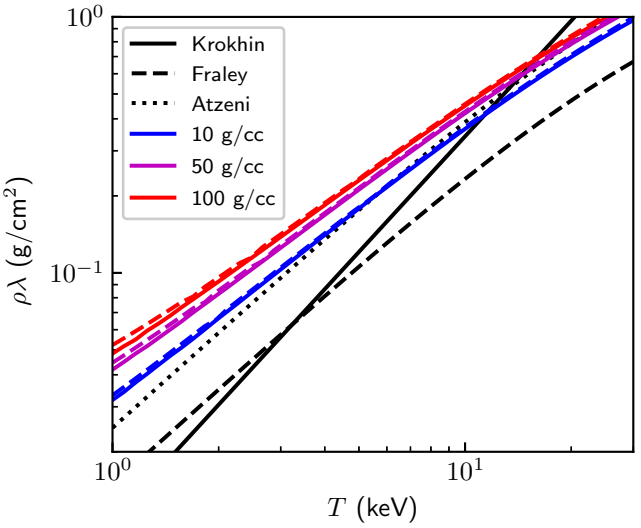

FIG. 2. Evaluations of $\rho\lambda$ using MD (solid) and BPS (dashed) at three densities compared to the Krokhin, Fraley, and Atzeni evaluations.

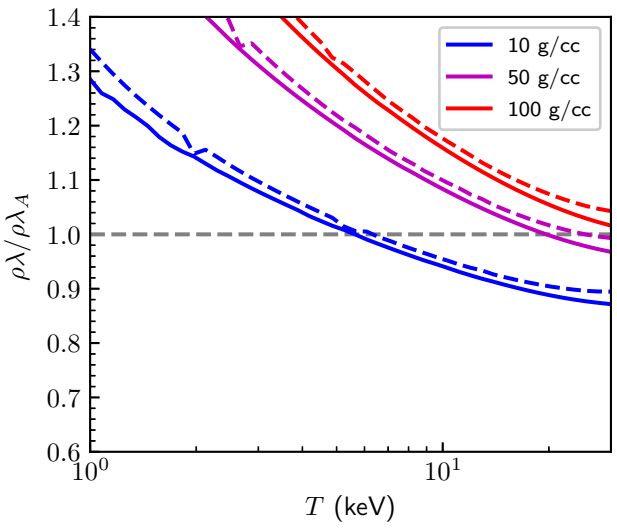

FIG. 3. MD (solid) and BPS (dashed) evaluated $\rho\lambda$ relative to Atzeni ($\rho\lambda_A$) versus temperature.

previously-published fits: Krokhin (black solid), Fraley (black dashed), and Atzeni (black dotted). Of these the Atzeni curve is clearly closest to our evaluations, although significant discrepancies exist depending on density and temperature.

The difference between our new evaluation and the Atzeni fit is shown in more detail in Fig. 3. We find that differences on the order of tens of percent can exist between evaluated α ranges using the MD and BPS theories and the fits using earlier and more simplified forms of dE/dx. However, the two theories for dE/dx, MD and BPS, give very similar results even though the underlying physics in the theories is markedly different. From here, we will use MD in all plotted evaluations, but give fit parameters for both models.

A challenge for any such evaluation is that the relevant parameter space for ρ and T can span orders of magnitude, both in terms of the variety of ICF designs and the range of parameter space accessed during an implosion's deceleration, stagnation, and expansion phases. The α transport quantities then ought to be accurate over a wide range of densities and temperatures. Color maps are shown in Fig. 4 of the α particle range for the four models (this work compared to Atzeni, Fraley, and Krokhin-Rozanov). The bottom row shows the difference between the previous three fits and our work with contours of 5 (red), 10 (purple), and 20 (white) percent. The Fraley fit is off by more than 20% for the entire plotted ρ, T space because of its low-density assumption. Atzeni and Krokhin-Rozanov are accurate but only over a narrow range of ρ, T.

We fit a simple expression to our numerical results for use in models. Similar to the form published by Fraley and Atzeni, but adding the possibility of a density dependence, we use the functional form

$$\rho\lambda = \frac{aT^c}{1+bT^c}\left(1+d\rho_{100}^e\right), \tag{12}$$

where a, b, c, d, and e are free parameters in the fit, T is the temperature in keV, and ρ_{100} is the mass density in units of 100 g/cc. The best-fit values are given in Table I using both the MD and BPS stopping powers.

TABLE I. Fit parameters for $\rho\lambda$

	MD	BPS
a	0.01705	0.01556
b	0.01133	0.007144
c	1.0706	1.0804
d	1.5793	1.7823
e	0.1987	0.2003

Figure 5 shows the relative difference between the fit value and the actual value for $\rho\lambda$ using the MD stopping power and the fit given by Eq. 12 and Table I. Over most of the parameter space relevant to hot-spot ignition, these fits are accurate to $\sim 2\%$.

IV. EFFICACY

The self-heating efficacy, f_α, is defined as the fraction of the α particle energy deposited into the hot spot. Given a uniform spherical hot spot with a specified density and temperature then f_α depends on the geometry and α particle dE/dx. The previously-published fits employ a basic geometric argument to calculate f_α. For example, Krokhin and Rozanov use,

$$f_\alpha = 1 - \frac{3}{2R^3}\int_0^R r^2 dr \int_{-1}^1 d\mu \left(1-\frac{\mathfrak{r}}{\rho\lambda}\right)^2 \tag{13}$$

where R is the radius of the hot spot, $\mu = \cos\theta$ and r are variables of integration, and $\mathfrak{r} = \rho\mu + \sqrt{R^2 - r^2(1-\mu^2)}$. This ex-

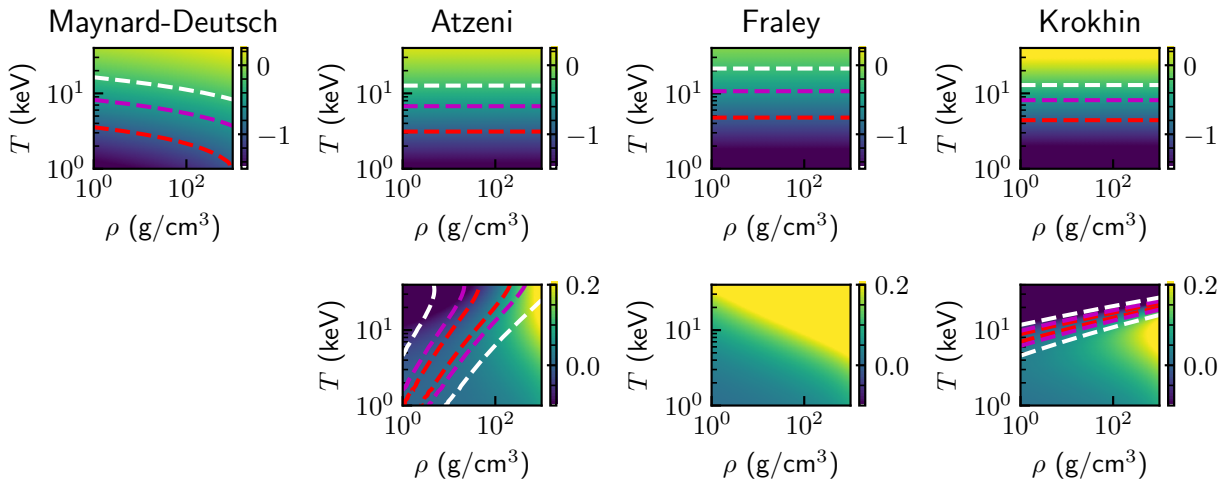

FIG. 4. Top: Colormaps of α particle range ($\rho\lambda$, top) for our evaluation using Maynard-Deutsch, Atzeni, Fraley, and Krokhin-Rozanov. The color scale is $\log_{10}(\rho\lambda)$ in unites of g/cm^2. Contours of 0.1 (red), 0.25 (magenta), and 0.5 (white) g/cm^2 are shown. Bottom: difference between the three previous fits and our evaluation, with contours of 5% (red), 10% (purple), and 20% (white).

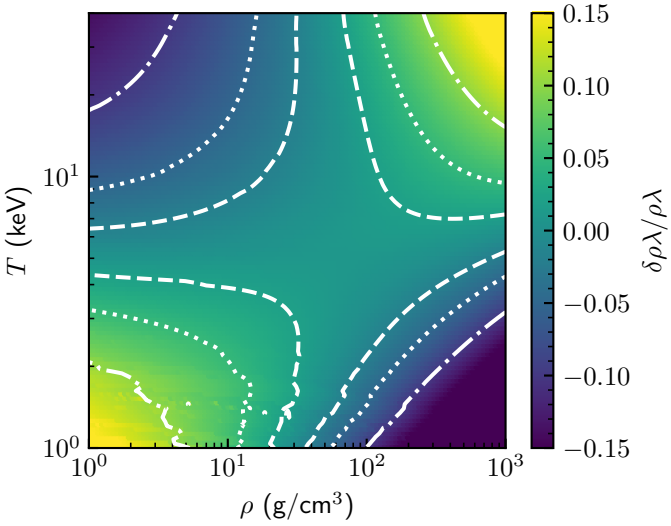

FIG. 5. Deviation of the fit from the actual value over ρ, T parameter space. Contours of 2% (dashed), 5% (dotted) and 10% (dash-dot) are shown.

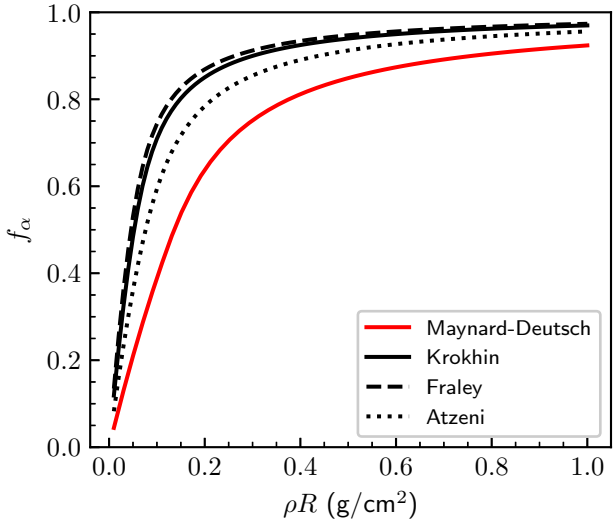

FIG. 6. f_α versus hot-spot ρR at 75 g/cc and 5 keV.

pression does not include the fact that the α particle deposits its energy non-uniformly along its range. We can account for this by invoking the range, and calculate an effective average α energy loss by

$$f_\alpha = \frac{3}{2R^3}\int_0^R r^2 dr \int_{-1}^{1} d\mu \frac{E_0(T) - E(T,L)}{E_0(T)} \qquad (14)$$

where $E(T,L)$ is the α energy after passing through a length L of plasma, where $L = r\mu + \sqrt{R^2 - r^2(1-\mu^2)}$.

Calculated values from Eq. 14 using the MD stopping power are shown in Fig. 6 compared to the previously-published fits. Our values are noticeably lower, especially for ρR values of a few hundred mg/cm^2, which are most relevant to hot-spot ignition. Current implosions on NIF achieve peak hot-spot ρRs of $\sim 0.2-0.3$ g/cm^2, where these calculated curves are the most different.

Next we evaluate f_α over an ICF-relevant parameter space of ρ (10-100 g/cc), T (1-10 keV), and ρR (0.05-0.5 g/cc). These calculations are shown in Fig. 7.

We fit the calculated f_α using a polynomial in $\rho\lambda/\rho R$, with $\rho\lambda$ calculated using the fit defined in the previous section (Eq. 12 and Table I). So,

$$f_\alpha = a - b\left(\frac{\rho\lambda}{\rho R}\right) + c\left(\frac{\rho\lambda}{\rho R}\right)^2 - d\left(\frac{\rho\lambda}{\rho R}\right)^3, \qquad (15)$$

where a, b, c, and d are the fit parameters. Coefficients for this

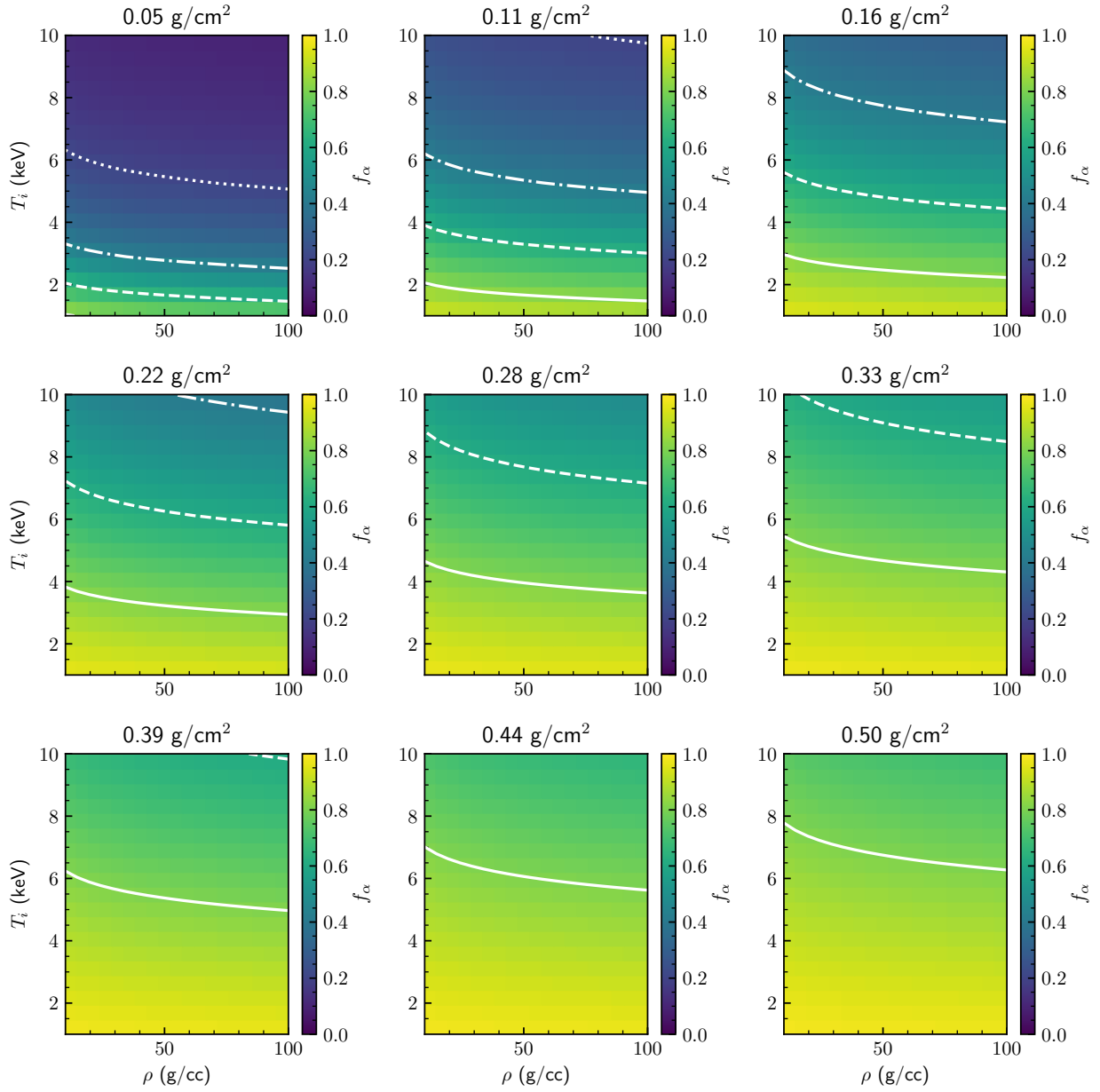

FIG. 7. Calculated f_α at various values of ρR versus T and ρ. Contours are shown at f_α values of 0.2 (dotted), 0.4 (dot-dash), 0.6 (dashed), and 0.8 (solid).

fit are given for both MD and BPS in Table II. The average error for this fit over the range of ρ, T, and ρR given above is 2.8% (2.7%) for the MD (BPS) stopping power.

TABLE II. Fit coefficients for f_α

	MD	BPS
a	1.0228	1.0145
b	0.4254	0.4105
c	0.07101	0.06579
d	0.00400	0.003522

V. ENERGY PARTITION

The energy partition between ions and electrons is calculated following Eq. 13 but tallying the ion and electron components separately, where the partition to electrons F_e is defined as the energy deposited to the electrons over the total energy lost. Previous calculations of the energy partition function often treat it as the energy partitioning for a ranged-out α particle in a plasma with given temperature and areal density greater than the α's range. This can break down for high-temperature hot spots with modest ρR, because the ion stopping is predominantly important towards the end of the

α particles range, yet the range increases with temperature (e.g. Fig. 3). So at temperatures where the energy partition is thought to be comparable to 50% (roughly 30 keV), the α range has increased to ~ 1 g/cm^2.

We fit the energy partition F_e with a function of both T and ρR,

$$F_e = \frac{a}{a+T_e}\left[1+b(\rho R)^c\right], \tag{16}$$

where a, b, and c are the fit coefficients, which are given in Table III for the MD and BPS stopping powers. T_e is in units of keV and ρR is in units of g/cm^2. These fits have an average error of 1.5% (1.7%) over the same parameter space used for the f_α fit. We note that our values for a are significantly larger than those reported by other authors, for example Atzeni's equivalent expression uses $a = 28$. This is because we consider the areal density dependence and ion stopping is unimportant at low areal density.

TABLE III. Fit coefficients for F_e

	MD	BPS
a	101	120
b	-0.2815	-0.2650
c	1.3615	1.1876

VI. EFFECT ON MODELS

We evaluate the effect of our new expression, specifically for f_α, using the analytic model described in Ref. 27. That paper, among others, present a simple condition that must be satisfied to achieve a burning plasma,

$$7.4\times10^{25} f_\alpha (\rho R)_{hs} \frac{\langle\sigma v\rangle}{T_{hs}} > v_{imp}, \tag{17}$$

which depends on the hot-spot areal density (ρR) and temperature (T), the DT fusion reactivity ($\langle\sigma v\rangle$), the implosion velocity (v_{imp}), and f_α. This expression corresponds to the parameter regimes where α self-heating is the dominant source of plasma heating. For a given implosion velocity, this expression can be used to draw the burning plasma regime's boundary on ρR, T space since f_α can be calculated based on ρ, ρR, and T. Reaching burning-plasma conditions on NIF is a major milestone that the program seeks to achieve, yet claiming that a burning plasma has been created relies upon these fundamental properties. Fig. 8 shows an updated version of the burning-plasma boundary plot given in Ref. 27, which used the Atzeni f_α (blue dashed curve), compared to an equivalent curve using our f_α (solid blue). Our curve shifts to a slightly higher requirement on ρR, which corresponds directly to the reduced heating efficacy in these calculations.The difference between the models is particularly notable given the location of the highest-performing implosions in ρ, T space. The data

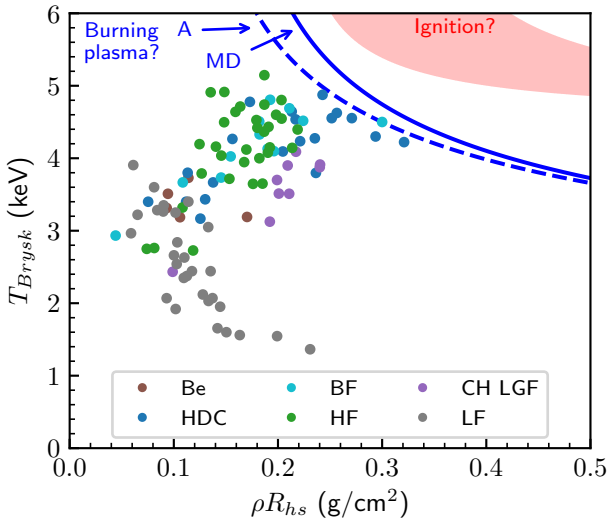

FIG. 8. ρR and T parameter space with a suite of implosions from different designs. The burning plasma condition using our model [solid blue (MD)] is noticeably farther from the data than the Atzeni curve [blue dashed (A)]. These are calculated at $v_{imp} = 400$ km/s. The BPS boundary is nearly identical to MD. The red shaded region is a depiction of the ignition boundary.

points in Fig. 8 (shown without uncertainty for clarity) represent a suite of different implosion designs conducted on NIF.

Similarly the ignition criterion is sensitive to the reduced α-heating efficacy, towards requiring higher ρR. The red region in Fig. 8 is a rough depiction of the uncertainty in the ignition boundary due to transport physics including this self-heating efficacy and other loss mechanisms, based on the model in Ref. 27. More work would be needed to rigorously define an efficacy-dependent ignition criterion.

We can explore the effect in more detail using the dynamic model described in Ref. 27. Three model runs with varying initializations are run with both the Atzeni model for f_α and our expression for f_α (using the MD stopping power). These are shown in Fig. 9, including both the implosion trajectory in ρR, T space (top) and the pressure versus time (bottom). In the trajectory plot the implosions advance in time clockwise along the curve starting at low ρR and T and beginning to self-heat as the temperature exceeds ~ 4 keV. The model's self-heating efficacy is substantially higher with the Atzeni f_α, and the hot spot reaches higher temperatures. Using the MD value for f_α results in a lower-temperature but higher-density hot spot, because the lower value of f_α allows slightly higher compression and increases the cold fuel ablation into the hot spot. Because of the lower temperature, the pressure is reduced.

Scalar quantities between the model runs with Atzeni and MD f_α are shown in Fig. 10. For a given model initialization, the MD f_α clearly gives lower yield, pressure, and ion temperature at roughly comparable hot-spot areal density. In order to match experiments, this may reduce the need to invoke additional loss mechanisms to analytic models (e.g. Ref.

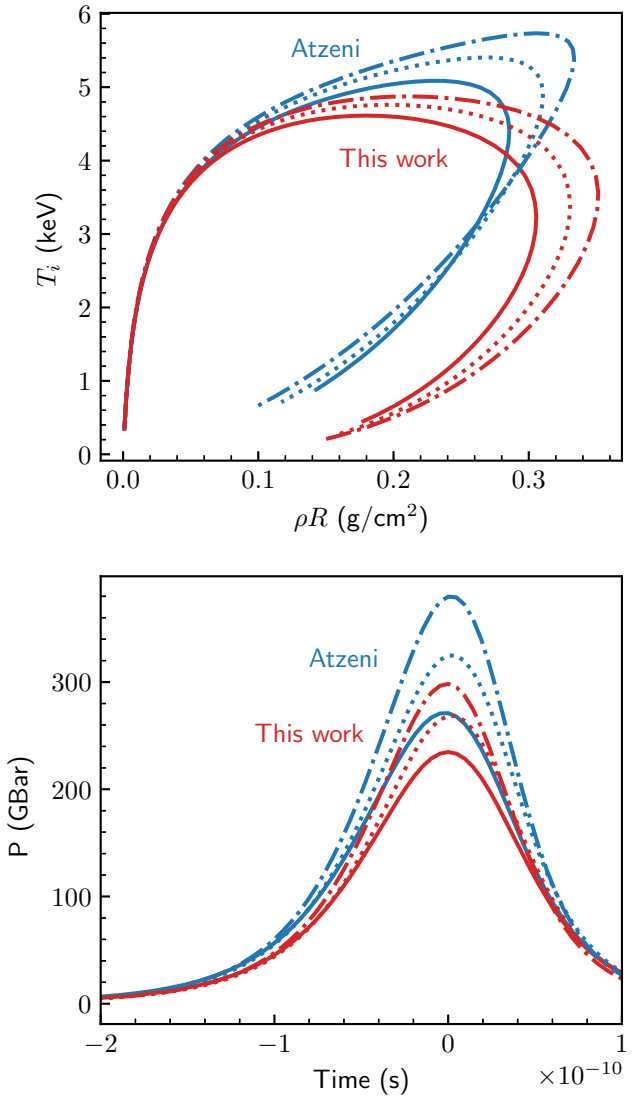

FIG. 9. Implosion trajectory in T_i, ρR space (top) and hot-spot pressure versus time (bottom) for three model initializations (solid, dotted, and dash-dot curves) run with either the Atzeni (blue) or MD (red) f_α.

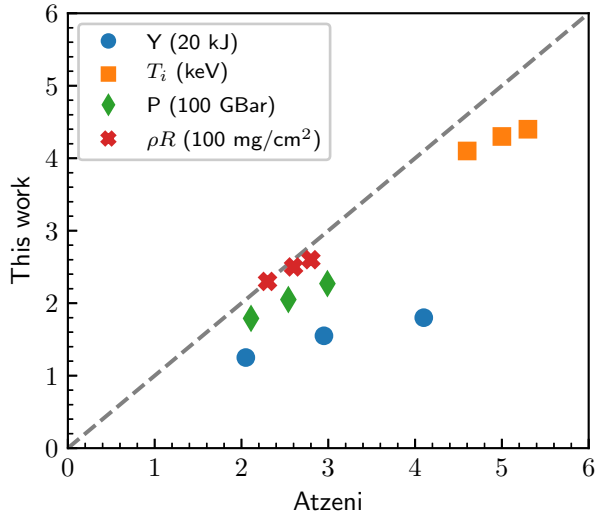

FIG. 10. Scalar quantities from the model runs using this work's MD fit for f_α compared to Atzeni. Shown are yield (in units of 20 kJ), temperature (in keV), pressure (in 100s of GBar), and hot-spot ρR (in 100s of mg/cm^2).

21), such as 3-D 'aneurysms' or mix, to explain the data. A more detailed evaluation of the current NIF database is needed but is beyond the scope of this paper.

We note that modern radiation-hydrodynamics simulations utilize modern dE/dx theory, typically a parameterized version of MD[34] and are unlikely to be affected to the same extent as recent analytic modeling. f_α is implicit in such a simulation through a charged-particle transport model. This includes 2-D and 3-D simulations, the latter of which are often close to experimental observables but take significant computational resources[?] .

This new parameterization for f_α can also affect data-based inferences of self-heating efficacy. For example in Ref. 6, the Atzeni expression is used to calculate f_α, and thus the total α-deposited energy, for three high-performing NIF shots. Using the three shots given in Table 1 of Ref. 6 we summarize the effect of using our model in Table IV. The T_i, P, and hot-spot ρR for N170601 and N170827 are as calculated in Ref. 6, but for N140304 we recalculate the hot-spot parameters using the more representative DD T_i (see Ref. 5). Given these parameters (and noting $P = 0.77\rho T_i$ in units of GBar, g/cc, and keV[21]), f_α is calculated using both the Atzeni formula and our expression. Our numbers are lower by about $0.11 - 0.14$.

VII. CONCLUSIONS

The inertial fusion program seeks to achieve a burning plasma and then ignition in the laboratory. Understanding and evaluating current indirect-drive hot-spot ignition experiments, which have significant self-heating but are thought to be short of the burning plasma regime. This has motivated significant work on analytic implosion models, which often supplement traditional post-shot analysis using radiation-hydrodynamics simulations. Analytic models use an efficacy for self-heating that parameterizes the fraction of α particle energy deposited into the hot spot. We report new parameterizations of the DT-α range, heating efficacy, and ion/electron energy partition using two modern stopping-power theories. Our results give lower heating efficacy, f_α, than parameterizations used in recent model papers. This results in a theoretical boundary for the burning plasma regime shifting to higher areal density, farther away from present experimental conditions. In dynamic models the new f_α results in lower temperature and lower pressure hot spots for a given initialization. Our results are consistent with sensitivity studies using radiation-hydrodynamics simulations[32] and straight eval-

TABLE IV. Data-inferred f_α for three high-performing NIF shots, as reported in Ref. 6, except using the more representative DD-inferred temperature for N140304 (see Ref. 5).

				f_α		
	T_i (keV)	P (GBar)	ρR (HS, g/cm^2)	Atzeni	This work	δf_α
N170601	4.5 ± 0.12	320 ± 40	0.26 ± 0.03	0.85 ± 0.02	0.73 ± 0.03	-0.12 ± 0.01
N170827	4.5 ± 0.15	360 ± 45	0.30 ± 0.03	0.87 ± 0.02	0.76 ± 0.03	-0.11 ± 0.01
N140304	4.74 ± 0.25	191 ± 33	0.19 ± 0.02	0.78 ± 0.03	0.64 ± 0.04	-0.14 ± 0.01

uations of the stopping power[33]. Increasing the fidelity of microphysics used in these analytic models, such as in this work, is important for the ICF program's evaluation of our current status and path forward.

ACKNOWLEDGMENTS

This work was performed under the auspices of the U.S. Department of Energy by Lawrence Livermore National Laboratory in part under Contract DE-AC52-07NA27344.

[1] J. D. Lawson, Proceedings of the physical society. Section B **70**, 6 (1957).
[2] J. Nuckolls, L. Wood, A. Thiessen, and G. Zimmerman, Nature **239**, 139–142 (1972).
[3] G. Miller, E. Moses, and C. Wuest, Nuclear Fusion **44**, S228 (2004).
[4] O. Hurricane, D. Callahan, D. Casey, P. Celliers, C. Cerjan, E. Dewald, T. Dittrich, T. Döppner, D. Hinkel, L. Berzak Hopkins, J. Kline, S. Le Pape, T. Ma, A. MacPhee, J. Milovich, A. Pak, H.-S. Park, P. Patel, B. Remington, J. Salmonson, P. Springer, and R. Tommasini, Nature **506**, 343 (2014).
[5] O. Hurricane, D. Callahan, D. Casey, E. Dewald, T. Dittrich, T. Döppner, S. Haan, D. Hinkel, L. B. Hopkins, O. Jones, A. Kritcher, S. Le Pape, T. Ma, A. MacPhee, J. Milovich, J. Moody, A. Pak, H.-S. Park, P. Patel, J. Ralph, H. Robey, J. Ross, J. Salmonson, B. Spears, P. Springer, R. Tommasini, F. Albert, L. Benedetti, R. Bionta, E. Bond, D. Bradley, J. Caggiano, P. Celliers, C. Cerjan, J. Church, R. Dylla-Spears, D. Edgell, M. Edwards, D. Fittinghoff, M. Barrios Garcia, A. Hamza, R. Hatarik, H. Herrmann, M. Hohenberger, D. Hoover, J. Kline, G. Kyrala, B. Kozioziemski, G. Grim, J. Field, J. Frenje, N. Izumi, M. Gatu Johnson, S. Khan, J. Knauer, T. Kohut, O. Landen, F. Merrill, P. Michel, A. Moore, S. Nagel, A. Nikroo, T. Parham, R. Rygg, D. Sayre, M. Schneider, D. Shaughnessy, D. Strozzi, R. Town, D. Turnbull, P. Volegov, A. Wan, K. Widmann, C. Wilde, and C. Yeamans, Nature Physics **12**, 800 (2016).
[6] S. Le Pape, L. F. Berzak Hopkins, L. Divol, A. Pak, E. L. Dewald, S. Bhandarkar, L. R. Bennedetti, T. Bunn, J. Biener, J. Crippen, D. Casey, D. Edgell, D. N. Fittinghoff, M. Gatu-Johnson, C. Goyon, S. Haan, R. Hatarik, M. Havre, D. D.-M. Ho, N. Izumi, J. Jaquez, S. F. Khan, G. A. Kyrala, T. Ma, A. J. Mackinnon, A. G. MacPhee, B. J. MacGowan, N. B. Meezan, J. Milovich, M. Millot, P. Michel, S. R. Nagel, A. Nikroo, P. Patel, J. Ralph, J. S. Ross, N. G. Rice, D. Strozzi, M. Stadermann, P. Volegov, C. Yeamans, C. Weber, C. Wild, D. Callahan, and O. A. Hurricane, Phys. Rev. Lett. **120**, 245003 (2018).
[7] A. B. Zylstra, J. A. Frenje, P. E. Grabowski, C. K. Li, G. W. Collins, P. Fitzsimmons, S. Glenzer, F. Graziani, S. B. Hansen, S. X. Hu, M. G. Johnson, P. Keiter, H. Reynolds, J. R. Rygg, F. H. Séguin, and R. D. Petrasso, Phys. Rev. Lett. **114**, 215002 (2015).
[8] J. A. Frenje, P. E. Grabowski, C. K. Li, F. H. Séguin, A. B. Zylstra, M. Gatu Johnson, R. D. Petrasso, V. Y. Glebov, and T. C. Sangster, Phys. Rev. Lett. **115**, 205001 (2015).
[9] A. C. Hayes, G. Jungman, A. E. Schulz, M. Boswell, M. M. Fowler, G. Grim, A. Klein, R. S. Rundberg, J. B. Wilhelmy, D. Wilson, C. Cerjan, D. Schneider, S. M. Sepke, A. Tonchev, and C. Yeamans, Physics of Plasmas **22**, 082703 (2015).
[10] W. Cayzac, A. Frank, A. Ortner, V. Bagnoud, M. Basko, S. Bedacht, C. Bläser, A. Blažević, S. Busold, O. Deppert, J. Ding, M. Ehret, P. Fiala, S. Frydrych, D. Gericke, L. Hallo, J. Helfrich, D. Jahn, E. Kjartansson, A. Knetsch, D. Kraus, G. Malka, N. Neumann, K. Pepitone, D. Pepler, S. Sander, G. Schaumann, T. Schlengel, N. Schroeter, D. Schumacher, M. Seibert, A. Tauschwitz, J. Vorberger, F. Wagner, S. Weih, Y. Zobus, and M. Roth, Nature communications **8**, 15693 (2017).
[11] J. A. Frenje, R. Florido, R. Mancini, T. Nagayama, P. E. Grabowski, H. Rinderknecht, H. Sio, A. Zylstra, M. Gatu Johnson, C. K. Li, F. H. Séguin, R. D. Petrasso, V. Y. Glebov, and S. P. Regan, Phys. Rev. Lett. **122**, 015002 (2019).
[12] G. Maynard and C. Deutsch, Phys. Rev. A **26**, 665 (1982).
[13] G. Maynard and C. Deutsch, J. Physique **46**, 1113–1122 (1985).
[14] L. S. Brown, D. L. Preston, and R. L. Singleton Jr., Physics Reports **410**, 237 – 333 (2005).
[15] J. D. Lindl, *Inertial confinement fusion: the quest for ignition and energy gain using indirect drive* (American Institute of Physics, 1998).
[16] C. D. Zhou and R. Betti, Phys. Plasmas **15**, 102707 (2008).
[17] R. Betti, P. Y. Chang, B. K. Spears, K. S. Anderson, J. Edwards, M. Fatenejad, J. D. Lindl, R. L. McCrory, R. Nora, and D. Shvarts, Phys. Plasmas **17**, 058102 (2010).
[18] C. Cerjan, P. T. Springer, and S. M. Sepke, "Integrated diagnostic analysis of inertial confinement fusion capsule performance," Phys. Plasmas **20**, 056319 (2013).
[19] R. Betti, A. R. Christopherson, B. K. Spears, R. Nora, A. Bose, J. Howard, K. M. Woo, M. J. Edwards, and J. Sanz, Phys. Rev. Lett. **114**, 255003 (2015).
[20] O. A. Hurricane, A. Kritcher, D. A. Callahan, O. Landen, P. K. Patel, P. T. Springer, D. T. Casey, E. L. Dewald, T. R. Dittrich, T. Döppner, D. E. Hinkel, L. F. Berzak Hopkins, J. Kline, S. Le Pape, T. Ma, A. G. MacPhee, A. Moore, A. Pak, H.-S. Park, J. Ralph, J. D. Salmonson, and K. Widmann, Phys. Plasmas **24**, 092706 (2017).
[21] P. Springer, O. Hurricane, J. Hammer, R. Betti, D. Callahan, E. Campbell, D. Casey, C. Cerjan, D. Cao, E. Dewald, L. Divol, T. Doeppner, M. Edwards, J. Field, C. Forrest, J. Frenje, J. Gaffney, M. Gatu-Johnson, V. Glebov, V. Goncharov, G. Grim, E. Hartouni, R. Hatarik, D. Hinkel, L. B. Hopkins, I. Igumenshchev, P. Knapp, J. Knauer, A. Kritcher, O. Landen, A. Pak, S. L. Pape, T. Ma, A. MacPhee, D. Munro, R. Nora, P. Patel, L. Peterson, P. Radha, S. Regan, H. Rinderknecht, C. Sangster, B. Spears, and C. Stoeckl, Nuclear Fusion **59**, 032009 (2018).
[22] O. A. Hurricane, D. A. Callahan, P. T. Springer, M. J. Edwards, P. Patel, K. Baker, D. T. Casey, L. Divol, T. Döppner, D. E. Hinkel, L. F. B. Hopkins, A. Kritcher, S. L. Pape, S. Maclaren, L. Masse, A. Pak, L. Pickworth, J. Ralph, C. Thomas, A. Yi, and A. Zylstra, Plasma Phys. Control. Fusion **61**, 014033 (2018).
[23] A. R. Christopherson, R. Betti, A. Bose, J. Howard, K. M. Woo, E. M. Campbell, J. Sanz, and B. K. Spears, Phys. Plasmas **25**, 012703 (2018).
[24] A. R. Christopherson, R. Betti, J. Howard, K. M. Woo, A. Bose, E. M. Campbell, and V. Gopalaswamy, Phys. Plasmas **25**, 072704 (2018).
[25] J. D. Lindl, S. W. Haan, O. L. Landen, A. R. Christopherson, and R. Betti, Phys. Plasmas **25**, 122704 (2018).
[26] A. R. Christopherson, R. Betti, and J. D. Lindl, Phys. Rev. E **99**, 021201 (2019).
[27] O. Hurricane *et al.*, "Approaching a burning plasma on the NIF," accepted by Phys. Plasmas (2019).
[28] O. N. Krokhin and V. B. Rozanov, Kvantovaya Elektronika , 118–120 (1972).
[29] G. Fraley, E. Linnebur, R. Mason, and R. Morse, Phys. Fluids **17**, 474–489 (1974).

[30]S. Atzeni and J. Meyer-Ter-Vehn, *The Physics of Inertial Fusion: Beam Plasma Interaction, Hydrodynamics, Hot Dense Matter*, International Series of Monographs on Physics (Oxford University Press, 2004).
[31]A. Zylstra, *Using fusion-product spectroscopy to study inertial fusion implosions, stopping power, and astrophysical nucleosynthesis at OMEGA and the NIF*, Ph.D. thesis, Massachusetts Institute of Technology (2015).
[32]M. Temporal, B. Canaud, W. Cayzac, R. Ramis, and R. L. Singleton, The European Physical Journal D **71**, 132 (2017).
[33]R. L. Singleton, Phys. Plasmas **15**, 056302 (2008).
[34]G. Zimmerman, "Recent Developments in Monte Carlo Techniques," LLNL report, UCRL-JC-105616 (1990).